DOI: 10.1021/ic100556p

Inorganic Chemistry
Article

Exchange-Coupled Cobalt(II) Dimer with Unusual Magnetic Circular Dichroism Saturation Behavior

S. Ostrovsky,[†,‡] Z. Tomkowicz,[†,§] and W. Haase*[,†]

[†]*Eduard-Zintl-Institute of Inorganic and Physical Chemistry, Darmstadt University of Technology, Petersenstrasse 20, 64287 Darmstadt, Germany,* [‡]*Institute of Applied Physics, Academy of Sciences of Moldova, Academy 5, MD-2028 Chisinau, Moldova, and* [§]*Institute of Physics, Jagiellonian University, Reymonta 4, 30-059 Kraków, Poland*

Received March 24, 2010

The exchange-coupled complex $[Co_2(\mu\text{-}H_2O)(\mu\text{-}OAc)_2(OAc)_2(tmen)_2]$ (OAc = CH_3COO^- acetato; tmen = *N*,*N*,*N*′,*N*′-tetramethylenediamine) has been studied by magnetic circular dichroism (MCD) spectroscopy and magnetization measurements. A peculiar behavior of the MCD spectra was observed with a change in the magnetic field. The intensity of particular lines initially increases, then decreases with an increase in the magnetic field strength, disappears with a further field increase, and appears again with the opposite sign. This behavior was explained by the overlap of the electronic transitions at different but near wavelengths. The obtained MCD magnetization curves, together with magnetization obtained by a SQUID magnetometer, are well reproduced using the Hamiltonian, which takes into account an orbital magnetic moment.

Introduction

Over the last years, magnetic circular dichroism (MCD) spectroscopy has been intensively used for the characterization of exchange-coupled high-spin cobalt(II) systems.[1−6] The MCD spectra for a variety of cobalt(II) monomers and exchange-coupled cobalt(II) dimers and trimers can be found in a review article.[7] In a continuation of our recent variable-temperature, variable-field (VTVH) MCD and magnetization studies on several octahedrally coordinated high-spin cobalt(II) monomers and oligomers, we focused on some water- and double-acetato-group-bridged high-spin cobalt(II) dimers. Those complexes belong in a broader sense to the class of dinuclear metallohydrolases, which are an important group of metalloenzymes catalyzing the hydrolysis of a range of peptide and phosphate ester bonds.[6] Amidohydrolases, amidinohydrolases, and peptide hydrolases belonging to them possess the common structural unit of a dinuclear metal active site featuring zinc(II), nickel(II), cobalt(II), and manganese(II), which occur respectively in leucine aminopeptidase, urease, methionine aminopeptidase, and arginase.[8−10] Nowadays, there is a growing interest in the characterization, modeling, and theoretical description of such compounds.

The case of two or more exchange-coupled high-spin Co^{II} ions in the octahedral surroundings is the most interesting; however, its theoretical treatment is somewhat complicated because the $^4T_{1g}$ ground state is orbitally degenerate and, in general, the orbital angular momentum should be included in the consideration.[11] For real compounds, distortion occurs and the symmetry of the Co^{II} ions is, at best, axial. In the case when the octahedron is strongly elongated, the orbital angular momentum disappears and the magnetic behavior of the studied complex can usually be explained using the ordinary spin Hamiltonian with zero-field splitting. In our previous study[12] of the title compound $[Co_2(\mu\text{-}H_2O)(\mu\text{-}OAc)_2(OAc)_2(tmen)_2]$, such an analysis based on the spin Hamiltonian

*To whom correspondence should be addressed. E-mail: haase@chemie.tu-darmstadt.de.

(1) Larrabee, J. A.; Johnson, W. R.; Volwiler, A. S. *Inorg. Chem.* **2009**, *48*, 8822–8829.
(2) Tomkowicz, Z.; Ostrovsky, S.; Haase, W. *Inorg. Chem.* **2008**, *47*, 6956–6963.
(3) Larrabee, J. A.; Chyun, S. A.; Volwiler, A. S. *Inorg. Chem.* **2008**, *47*, 10499–10508.
(4) Johansson, F. B.; Bond, A. D.; Nielsen, U. G.; Moubaraki, B.; Murray, K. S.; Berry, K. J.; Larrabee, J. A.; McKenzie, C. J. *Inorg. Chem.* **2008**, *47*, 5079–5092.
(5) Ostrovsky, S. M.; Falk, K.; Pelikan, J.; Brown, D. A.; Tomkowicz, Z.; Haase, W. *Inorg. Chem.* **2006**, *45*, 688–694.
(6) Xavier, F. R.; Neves, A.; Casellato, A.; Peralta, R. A.; Bortoluzzi, A. J.; Szpoganicz, B.; Severino, P. C.; Terenzi, H.; Tomkowicz, Z.; Ostrovsky, S.; Haase, W.; Ozarowski, A.; Krzystek, J.; Telser, J.; Schenk, G.; Gahan, L. R. *Inorg. Chem.* **2009**, *48*, 7905–7921.
(7) Ostrovsky, S.; Tomkowicz, Z.; Haase, W. *Coord. Chem. Rev.* **2009**, *253*, 2363.
(8) Beckett, R. P.; Davidson, A. H.; Drummond, A. H.; Huxley, P.; Whitetaker, M. *Drug Discovery Today* **1996**, *1*, 16.
(9) Dixon, N. E.; Reddles, P. W.; Gazzola, C.; Blakeley, R. L.; Zerner, B. *Can. J. Biochem.* **1980**, *58*, 1335.
(10) Arnold, M.; Brown, D. A.; Deeg, O.; Errington, W.; Haase, W.; Herlihy, K.; Kemp, T. J.; Nimir, H.; Werner, R. *Inorg. Chem.* **1998**, *37*, 2920.
(11) Lloret, F.; Julve, M.; Cano, J.; Ruiz-García, R.; Pardo, E. *Inorg. Chim. Acta* **2008**, *361*, 3432.
(12) Ostrovsky, S. M.; Werner, R.; Brown, D. A.; Haase, W. *Chem. Phys. Lett.* **2002**, *353*, 290.

Published on Web 07/07/2010

reproduced well the temperature dependence of the effective magnetic moment. No field-dependent magnetization measurements have been undertaken in that work.

In the present work, the study of the $[Co_2(\mu\text{-}H_2O)(\mu\text{-}OAc)_2(OAc)_2(tmen)_2]$ compound is continued using MCD spectroscopy. Magnetic measurements were repeated and completed with the field-dependent magnetization. It was observed that MCD spectra show a peculiar behavior with a change in the strength of the magnetic field. Usually, an increase of the external magnetic field leads to an increase of the MCD signal. However, in the case of the studied compound, the MCD intensity initially increases for some wavelengths with growth of the external magnetic field, passes through the maximum, and decreases. A further increase of the magnetic field even leads to a change of the sign of the MCD signal. This type of behavior of the MCD signal, in general, can appear in heteronuclear systems because different kinds of ions can give signals at the same wavelength but with opposite signs of the MCD *C* terms and with different dependences on the temperature and magnetic field. However, for the homonuclear symmetrical dimer, this type of behavior looks very strange. As will be shown below, the obtained data on MCD and magnetization demonstrate that the spin Hamiltonian, used in the previous stage of investigation, is not applicable for the full explanation of the magnetooptical behavior of this compound, and the orbital angular momentum should be included in the consideration.

Experimental Section

Synthesis. The details of the synthesis of the $[Co_2(\mu\text{-}H_2O)(\mu\text{-}OAc)_2(OAc)_2(tmen)_2]$ complex can be found elsewhere.[13]

MCD Spectroscopy. MCD spectra of the studied complex were collected by means of a Jasco J-810 spectropolarimeter, interfaced with an Oxford Instruments Spectromag SM 4000-9T optical cryostat equipped with a superconducting magnet. The samples were ground, and the obtained fine powder was mixed with Nujol. The MCD spectra were corrected for natural circular dichroism and other baseline effects by subtracting the background line at 0 T. Spectra were measured for various temperatures (3, 4, 5, 7, 10, 15, and 25 K) and, at each temperature, for various magnetic fields from 0 up to 8 T. The direction of the magnetic field was antiparallel to the beam direction (in discord with the now established convention).

Magnetic Measurements. Direct-current magnetization data were obtained with a SQUID magnetometer on a polycrystalline sample. The temperature dependence was measured at a field of 1000 Oe, and the field dependence was measured at 1.8 K. The sample was pressed into a pellet in order to avoid reorientation of the particles in a strong external magnetic field. The data were corrected for the diamagnetic core contribution using a Pascal's constants table.

Model for Theoretical Analysis

The crystal structure of the studied cobalt(II) complex was determined by Turpeinen et al.[13] This structure belongs to the orthorhombic space group *Pbca*. Figure 1 shows the molecular structure. The molecular symmetry is pseudo-C_{2v}. The summary formula is $C_{20}H_{46}Co_2N_4O_9$. Each cobalt ion is octahedrally coordinated, but the site symmetry is lower because of some distortion in the surroundings. The magnetic interaction between two metal ions takes place through two bridging acetates and one molecule of water.

(13) Turpeinen, U.; Ahlgren, M.; Hamalainen, R. *Acta Crystallogr., Sect. B* **1982**, *38*, 1580.

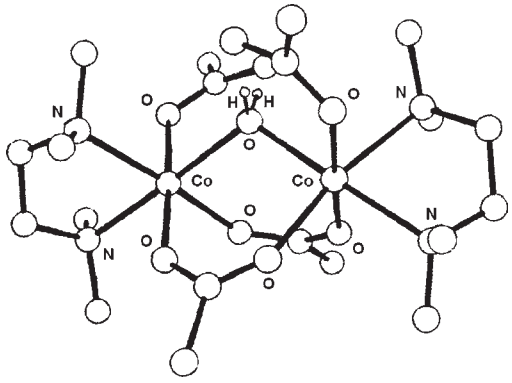

Figure 1. Structure of $[Co_2(\mu\text{-}H_2O)(\mu\text{-}OAc)_2(OAc)_2(tmen)_2]$ (adapted from ref 13). Hydrogen ions, except water hydrogen ions, are omitted for clarity.

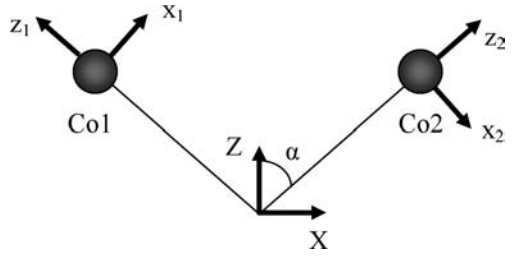

Figure 2. Molecular (*XYZ*) and local ($x_iy_iz_i$) coordinate systems (the *Y* and y_i axes are perpendicular to the figure surface).

The theoretical model used for analysis of the experimental data is widely described in ref 7. We recall it shortly with needed modifications. This model is based on the following Hamiltonian:

$$\mathbf{H} = \mathbf{H}_{SO} + \mathbf{H}_{Cr} + \mathbf{H}_{ex} + \mathbf{H}_{Ze} \quad (1)$$

The first term represents the spin−orbit coupling $\mathbf{H}^i_{SO} = -(3/2)\kappa\lambda\mathbf{S}_i\mathbf{L}_i$ ($i = 1, 2$), κ is the orbital reduction factor, and $\lambda = -170\ cm^{-1}$ is the spin−orbit coupling parameter for a free Co^{II} ion. The term $\mathbf{H}_{Cr}$ is due to lowering of the symmetry of the crystal field. It has the form $\mathbf{H}^i_{Cr} = \mathbf{L}_i\mathbf{\Delta}_i\mathbf{L}_i$ ($i = 1, 2$), where the $\mathbf{\Delta}_i$ tensor describes the splitting of the $^4T_{1g}$ term in the local crystal field. To avoid overparameterization, we assume that distortion from the octahedral symmetry is axial. In general, the main axes of the $\mathbf{\Delta}_i$ tensors belonging to different Co^{II} ions are not parallel. For calculation of the matrix elements of the $\mathbf{H}^i_{Cr}$ operators, we introduced the molecular coordinate system as shown in Figure 2. The local $\mathbf{\Delta}_i$ tensors in this molecular coordinate system can be obtained by unitary transformation (clockwise rotation of one ion and anticlockwise rotation of another one around the *Y* axis by half of the angle between local z_i axes):

$$\Delta_i = \begin{pmatrix} \Delta(\sin^2\alpha - 1/3) & 0 & \pm\Delta\sin\alpha\cos\alpha \\ 0 & -\Delta/3 & 0 \\ \pm\Delta\sin\alpha\cos\alpha & 0 & \Delta(\cos^2\alpha - 1/3) \end{pmatrix} \quad (i = 1, 2) \quad (2)$$

where Δ is the axial parameter of the local $\mathbf{\Delta}_i$ tensors (it is assumed that the axial parameters for both tensors are equal).

The third term in the Hamiltonian equation (1) represents the magnetic exchange between two cobalt ions. Under some assumptions, we can express it as[7,14,15]

$$\mathbf{H}_{ex} = -2J_{ex}\mathbf{S}_1\mathbf{S}_2 \quad (3)$$

The last term in eq 1 is the Zeeman interaction. It consists of both spin and orbital contributions and is

$$\mathbf{H}^i_{Ze} = \mu_B\left(g_0\mathbf{S}_i - \frac{3}{2}\kappa L_i\right)\mathbf{H} \quad (i = 1, 2) \quad (4)$$

where μ_B is the Bohr magneton and $g_0 = 2.0023$ is the free electron Landé factor. After the spin−orbit interaction between the $^4T_{1g}$ ground and excited states is accounted for, g_0 in eq 4 should be replaced by some averaged g value ranging between 2 and 2.12.[16]

The values of the magnetization and magnetic susceptibility for an arbitrary direction of the applied magnetic field are calculated in a standard way:

$$M(\vartheta, \varphi) = N_A k_B T \frac{\partial}{\partial H(\vartheta, \varphi)}\{\ln Z[H(\vartheta, \varphi)]\} \quad (5)$$

$$\chi(\vartheta, \varphi) = M(\vartheta, \varphi)/H(\vartheta, \varphi) \quad (6)$$

Z is the partition function and k_B and N_A are Boltzmann's constant and Avogadro's number, respectively. Angles ϑ and φ describe the orientation of the magnetic field with respect to the molecule-fixed coordinate system.

A general formula for analysis of the MCD spectra requires calculation of the difference between the molar extinction coefficients for the left and right circularly polarized light, i.e., $\Delta\varepsilon = \varepsilon_L - \varepsilon_R$. In the case of mononuclear complexes with orbitally degenerate ground states, the MCD saturation behavior depends on polarization of the corresponding transitions and can be simulated as[17]

$$\Delta\varepsilon(\vartheta, \varphi) \propto M_{xy}\cos\vartheta\langle L^z\rangle_T + M_{xz}\sin\vartheta\sin\varphi\langle L^y\rangle_T + M_{yz}\sin\vartheta\cos\varphi\langle L^x\rangle_T \quad (7)$$

where M_{ij} is a combination of the matrix elements of the ith and jth components of the electric dipole operator and $\langle L^k\rangle_T$ is the thermally averaged component of the orbital angular momentum within the ground state:

$$\langle L^k\rangle_T = \frac{1}{Z}\sum_a \langle a|L^k|a\rangle \exp(-E_a/k_BT), \quad k = x, y, z \quad (8)$$

where a represents the sublevels of the ground state. To obtain the signal from the randomly oriented molecules, eq 7 is integrated over all magnetic field orientations.

Analysis of the MCD behavior of the exchange-coupled systems is a complicated topic. If the exchange parameter is relatively big, the energy spectrum of the system represents the groups of levels (multiplets) well separated from each other. At low temperatures ($k_BT \ll J_{ex}$), only the ground-state multiplet is thermally populated. Equation 7 can be applied to this ground-state multiplet and, as a consequence, to the whole system. Typical values of the J_{ex} parameter in the exchange-coupled cobalt(II) complexes are about several wave numbers and, in general, these complexes belong to weakly coupled systems. In the case of weak exchange-coupled complexes, eq 7 is not valid; however, for binuclear cobalt systems, the situation is favorable. At low temperatures, each Co^{II} ion can be treated as a pseudospin $^1/_2$ system. Exchange interaction couples these pseudospins to the states with the total angular momentum $J = 0$ and 1. Both states are thermally accessible; however, the state with $J = 0$ is a nonmagnetic one and does not contribute to the MCD C term. So, like in the case of strongly coupled systems, at low temperature, the $J = 1$ state is the only thermally populated multiplet that gives the MCD C term. Equation 7 can be applied to this $J = 1$ state and, as a consequence, to the whole dimer. Because of the anisotropy of the exchange interaction that operates within the restricted space of the direct product of the ground-state Kramers doublets, the $J = 1$ state is split and this affects the MCD saturation behavior. Because this anisotropy strongly depends on the magnitude and on the sign of the Δ parameter (single ion property), analysis of the MCD behavior at the lowest temperature region gives not only the value of the exchange parameter but also the information about the type and strength of distortion of the local surroundings.

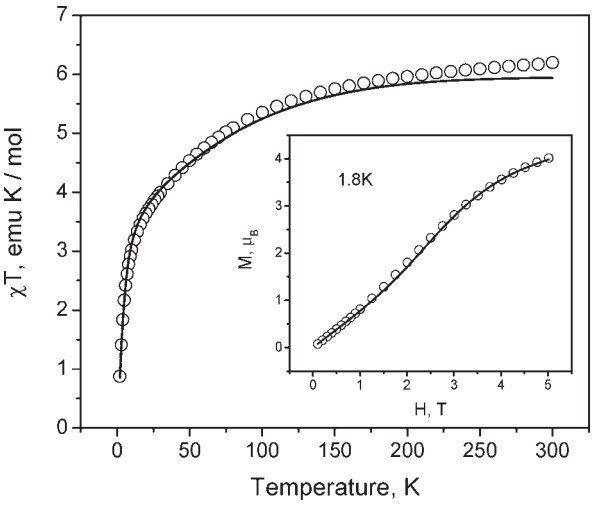

Figure 3. Experimental magnetic properties of $[Co_2(\mu\text{-}H_2O)(\mu\text{-}OAc)_2(OAc)_2(tmen)_2]$. Inset: magnetization vs field at 1.8 K. Theoretical curves are calculated at $\Delta = -870\,cm^{-1}$, $\kappa = 0.858$, $J_{ex} = -1.2\,cm^{-1}$, and $g = 2.03$.

Experimental Results and Their Analysis

The magnetic properties of the $[Co_2(\mu\text{-}H_2O)(\mu\text{-}OAc)_2(OAc)_2(tmen)_2]$ complex are presented in Figure 3. The main figure shows the temperature dependence of the χT product of susceptibility and temperature. In the inset, the field dependence of magnetization is presented. The value χT is about 6 emu·K·mol^{-1} at room temperature and decreases as the temperature decreases. The low temperature values of the χT product indicate an antiferromagnetic coupling between cobalt ions. Analysis of this behavior was performed on the basis of the model presented above. The best-fit parameters, obtained from analysis, are given in the figure caption. As can

(14) Lines, M. E. *J. Chem. Phys.* **1971**, *55*, 2977.
(15) Palii, A. V.; Tsukerblat, B. S.; Coronado, E.; Clemente-Juan, J. M.; Borras-Almenar, J. J. *Polyhedron* **2003**, *22*, 2537.
(16) Ostrovsky, S. M.; Falk, K.; Pelikan, J.; Brown, D. A.; Tomkowicz, Z.; Haase, W. *Inorg. Chem.* **2006**, *45*, 688.
(17) Oganesyan, V. S.; George, S. J.; Cheesman, M. R.; Thomson, A. J. *J. Chem. Phys.* **1999**, *110*, 762.

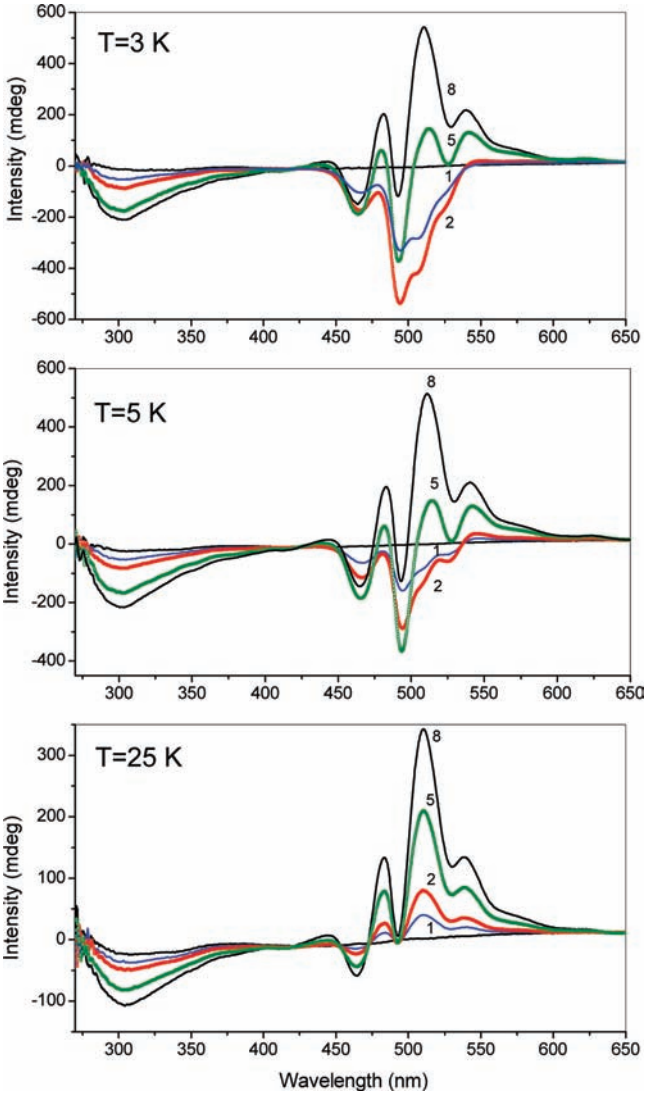

Figure 4. Experimental MCD spectrum of $[Co_2(\mu\text{-}H_2O)(\mu\text{-}OAc)_2(OAc)_2(tmen)_2]$ at 3, 5, and 25 K. Curve labels denote the magnetic field in Tesla.

be seen, a good agreement is obtained between the experimental data and theoretical modeling. A small negative value of the anisotropic exchange parameter is typical for the cobalt(II) complexes, where magnetic exchange takes place through the bridging water and carboxylate groups.[7,18] The obtained value of the orbital reduction factor lies between the limits for the weak and strong crystal fields and is also typical for high-spin cobalt(II) complexes.[7] A relatively large negative value of the Δ parameter indicates that distortion of the octahedral surroundings corresponds to compression along the symmetry axis. As mentioned in the Introduction, in the case of a strong distortion from the octahedral surrounding and a positive Δ parameter, the orbital angular momentum disappears and the system can be treated using the spin Hamiltonian with large values of the zero-field-splitting parameter. All attempts to explain the experimental magnetic data with a positive Δ value failed. So, one can conclude that the orbital angular momentum contribution is significant for the description of the behavior of the complex under study and cannot be excluded from the consideration.

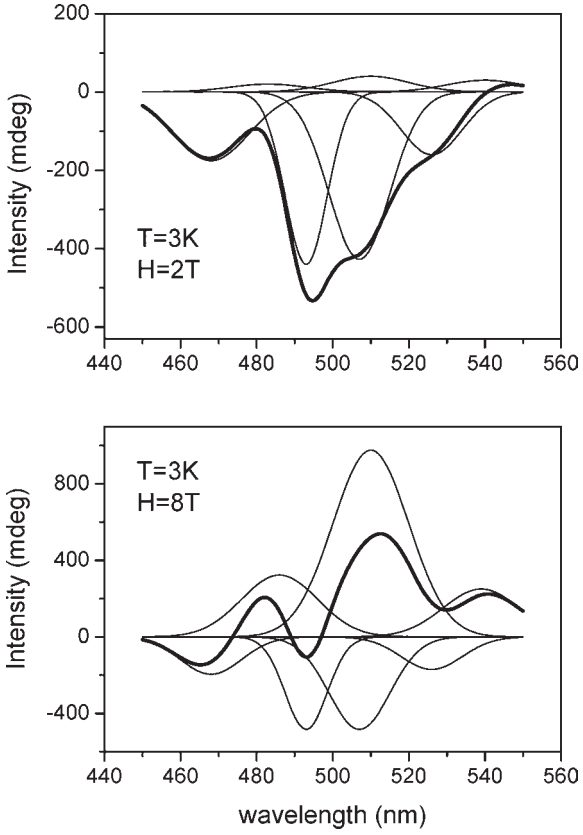

Figure 5. Gaussian deconvolution of the MCD spectrum of $[Co_2(\mu\text{-}H_2O)(\mu\text{-}OAc)_2(OAc)_2(tmen)_2]$ in the 450−550 nm spectroscopic region.

MCD spectra of the complex under investigation are shown in Figure 4. After a detailed examination of these spectra, one finds that, with a temperature increase, some peaks disappear. Another characteristic property of this spectrum is that at a given temperature an increase of the external magnetic field results in sign changes of the peaks at 488, 494, and 510 nm. This behavior, as was already mentioned, was not expected for homonuclear symmetric dimers. Nevertheless, it can be easily explained in the framework of our theoretical model. The MCD spectrum consists of several lines corresponding to different optical transitions. Each of these lines is rather broad and, in general, can overlap with the neighboring lines. The temperature and field behavior of the signal at any wavelength depends on the interplay between the lines corresponding to different optical transitions.

In the 450−550 nm spectroscopic region, the MCD spectrum of the investigated complex at any temperature and applied magnetic field can be simulated as a superposition of seven Gaussian lines. Lines located at 468, 493, 507, and 526 nm have negative intensity while ones at 485, 510, and 540 nm are positive. The corresponding Gaussian deconvolutions of the MCD spectra at 3 K and $H = 2$ and 8 T are shown in Figure 5. The widths of the Gaussian lines that form the spectrum range from 13 to 24 nm. We compared these values with the widths of the isolated lines in the MCD spectra of six-coordinated cobalt complexes in the same spectral region[19,20]

(18) Calvo-Perez, V.; Ostrovsky, S.; Vega, A.; Pelikan, J.; Spodine, E.; Haase, W. *Inorg. Chem.* **2006**, *45*, 644.

(19) Larrabee, J. A.; Leung, C. H.; Moore, R. L.; Thamrong-nawasawat, T.; Wessler, B. S. H. *J. Am. Chem. Soc.* **2004**, *126*, 12316–12324.

(20) Larrabee, J. A.; Alessi, C. M.; Asiedu, E. T.; Cook, J. O.; Hoerning, K. R.; Klingler, L. J.; Okin, G. S.; Santee, S. G.; Volkert, T. L. *J. Am. Chem. Soc.* **1997**, *119*, 4182–4196.

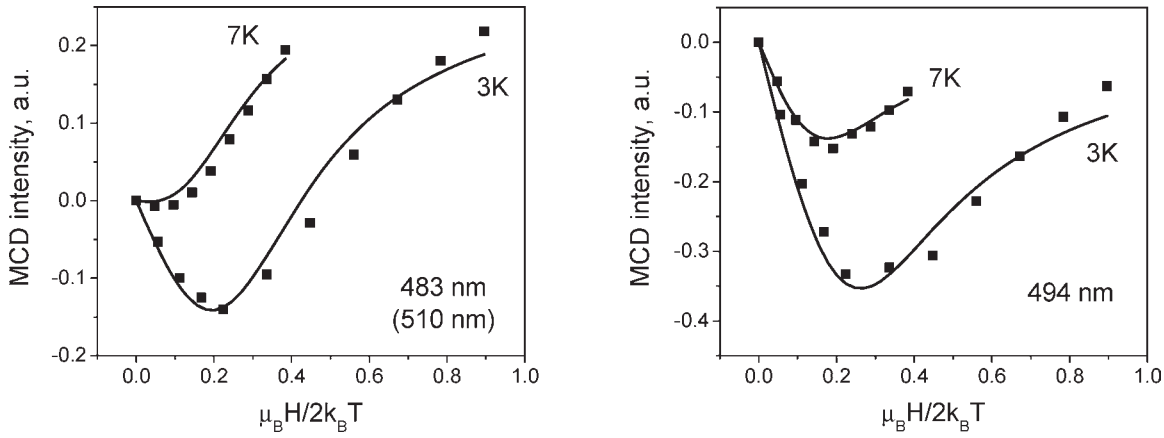

Figure 6. Magnetization curves recorded at 483 and 510 nm (left) and 494 nm (right). Theoretical curves are calculated with the use of eq 9 and with the set of best-fit parameters (see the caption for Figure 3).

and found that they are similar. It is seen that Gaussian lines in Figure 5 overlap each other, and at any wavelength, the MCD signal represents a superposition of different lines. For example, the signal at 494 nm is a result of four main contributions coming from lines centered at 485, 493, 507, and 510 nm.

The signal behavior at a given wavelength can be found as the sum of the corresponding contributions; each of these contributions is described by eq 7 with the corresponding M_{ij} values. This procedure was done for the signal intensities at 483, 494, and 510 nm, and the MCD saturation behavior at all of these wavelengths was analyzed considering different polarizations of the contributing optical transitions. It was found that the signal behavior at all three wavelengths can be well described with the assumption that the optical transitions with positive intensity are *xy*-polarized and the transitions with negative intensity are *yz*-polarized (the polarization of all optical transitions is given in the molecular coordinate system shown in Figure 2). As a result, the signal behavior at all three wavelengths can be simulated as a sum of two parts:

$$\Delta\varepsilon(\vartheta, \varphi, \lambda) \propto M_{xy}(\lambda) \cos \vartheta \langle L^z \rangle_T + M_{yz}(\lambda) \sin \vartheta \cos \varphi \langle L^x \rangle_T \quad (9)$$

with $M_{xy}(\lambda)$ being positive and $M_{yz}(\lambda)$ being negative. In eq 9, $M_{ij}(\lambda)$ parameters represent a sum of M_{ij} values from eq 7, with the summation being performed over all contributing transitions. The result of our theoretical simulation of the MCD saturation behavior is shown in Figure 6 as solid lines. In this simulation, the following relations between the $M_{ij}(\lambda)$ parameters in eq 9 were used: M_{xy} (494 nm)/M_{yz} (494 nm) = −1.4 and M_{xy} (483 nm)/M_{yz} (483 nm) = M_{xy} (510 nm)/M_{yz} (510 nm) = −2.2. One sees a very good agreement between the theoretical curves and the experimental points. The behavior of the MCD signals at all three wavelengths depends on two contributions of different signs. At low values of the external magnetic field, the negative contribution is larger and the resulting signal is negative. With a magnetic field increase, both positive and negative components start to change; however, the field dependence of these components is different. The positive one changes as a spatially and thermally averaged *z* component of the total orbital angular momentum, while the negative term behaves like an *x* component. As a result, at some value of the external magnetic field, the positive term becomes larger and the corresponding MCD signal disappears and appears again with the opposite sign with a further increase of the magnetic field.

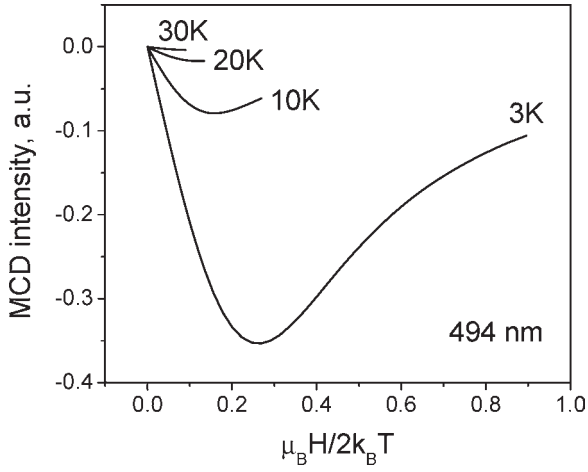

Figure 7. Theoretical simulation of the MCD magnetization curves at 494 nm.

The disappearance of some lines from the spectrum with a temperature increase has the same origin. To illustrate this, we modeled the MCD saturation behavior at 494 nm at different temperatures. The result is shown in Figure 7. At low temperatures, the signal is negative. With an increase of the external magnetic field, the absolute value of this signal initially increases, passes through the maximum, and starts to decrease. The temperature increase leads to a diminishing of the absolute value of the MCD signal. At 20 K, it is very small, and at a temperature of about 30 K and higher, the signal at 494 nm disappears because the positive and negative contributions to the signal cancel each other. This agrees well with the experimental data. As can be seen from Figure 4 at 25 K, the line at 494 nm with a negative sign of the signal practically disappears and, at higher temperatures, is not presented in the spectrum.

Summary

In this contribution, we reported the magnetooptical investigation of the exchange-coupled $[Co_2(\mu\text{-}H_2O)(\mu\text{-}OAc)_2(OAc)_2(tmen)_2]$ dimer. It was shown that, for the full description of the magnetic behavior and the determination of the key parameters

of the complex, the measurements of the temperature dependence of the susceptibility only are not sufficient. The results obtained in such a way may not be correct in some details. Additional measurements of the field dependence of the magnetization, done by a traditional and/or MCD technique, will be very useful for obtaining unambiguous results.

The observed peculiarities of the MCD behavior, namely, the disappearance of some lines with a magnetic field increase and the appearance again with the opposite sign, were explained by the overlap of the different electronic transitions.

It was shown that the description of the full magnetic and magnetooptical behavior was not possible within the spin-Hamiltonian formalism and the orbital angular momentum should be included in the consideration.

Acknowledgment. We thank Dr. M. Rams for magnetization measurements and the German Science Foundation, under Project Ha 782/85 (in the scope of Priority Project 1137 "Molecular Magnetism"), for the financial support.